J. Am. Soc. Mass Spectrom. (2018) 29:1416–1424
DOI: 10.1007/s13361-018-1947-5

RESEARCH ARTICLE

Influence of Background H_2O on the Collision-Induced Dissociation Products Generated from $[UO_2NO_3]^+$

Michael J. Van Stipdonk, Anna Iacovino, Irena Tatosian

Department of Chemistry, Duquesne University, 600 Forbes Avenue, Pittsburgh, PA 15282, USA

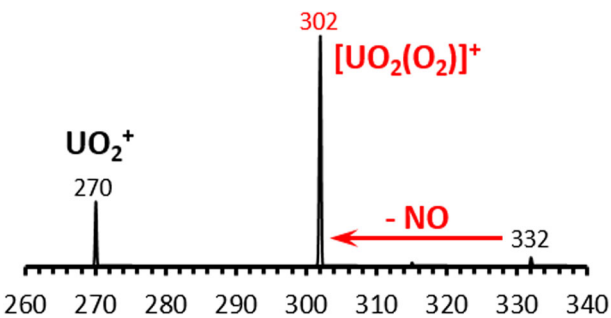

Abstract. Developing a comprehensive understanding of the reactivity of uranium-containing species remains an important goal in areas ranging from the development of nuclear fuel processing methods to studies of the migration and fate of the element in the environment. Electrospray ionization (ESI) is an effective way to generate gas-phase complexes containing uranium for subsequent studies of intrinsic structure and reactivity. Recent experiments by our group have demonstrated that the relatively low levels of residual H_2O in a 2-D, linear ion trap (LIT) make it possible to examine fragmentation pathways and reactions not observed in earlier studies conducted with 3-D ion traps (Van Stipdonk et al. J. Am. Soc. Mass Spectrom. **14**, 1205–1214, 2003). In the present study, we revisited the dissociation of complexes composed of uranyl nitrate cation $[U^{VI}O_2(NO_3)]^+$ coordinated by alcohol ligands (methanol and ethanol) using the 2-D LIT. With relatively low levels of background H_2O, collision-induced dissociation (CID) of $[U^{VI}O_2(NO_3)]^+$ primarily creates $[UO_2(O_2)]^+$ by the ejection of NO. However, CID (using He as collision gas) of $[U^{VI}O_2(NO_3)]^+$ creates $[UO_2(H_2O)]^+$ and UO_2^+ when the 2-D LIT is used with higher levels of background H_2O. Based on the results presented here, we propose that product ion spectrum in the previous experiments was the result of a two-step process: initial formation of $[U^{VI}O_2(O_2)]^+$ followed by rapid exchange of O_2 for H_2O by ion-molecule reaction. Our experiments illustrate the impact of residual H_2O in ion trap instruments on the product ions generated by CID and provide a more accurate description of the intrinsic dissociation pathway for $[U^{VI}O_2(NO_3)]^+$.

Keywords: Electrospray ionization, Uranyl, Collision-induced dissociation, Tandem mass spectrometry

Received: 21 February 2018/Revised: 18 March 2018/Accepted: 18 March 2018/Published Online: 13 April 2018

Introduction

Developing a comprehensive understanding of the reactivity of uranium species [1] remains important to the development of nuclear fuel processing methods [2] and studies of the migration and fate of the element in the environment [3, 4]. Electrospray ionization (ESI) is an effective tool for production of gas-phase complexes containing uranium in high oxidation states [5]. Our group was among the first to use ESI to generate gas-phase, doubly charged complexes containing the uranyl ion ($U^{VI}O_2^{2+}$) for studies of intrinsic structure and reactivity (i.e., outside of the influence of solvent or other condensed phase effects) in a species-specific fashion [6–15]. For example, ESI was used to generate the first complexes containing $U^{VI}O_2^{2+}$ coordinated by ligands such as acetone (aco) or acetonitrile (acn) for collision-induced dissociation (CID) and ion-molecule reaction experiments [6, 7]. Since then, ESI has been used to create gas-phase uranyl species for a range of tandem mass spectrometry, ion mobility, and anion photoelectron spectroscopy studies [16–41]. More recently, ESI and tandem mass spectrometry have been used to study and compare the reactivity of transuranic species [42–50]. For example, ESI was used to produce acn and aco complexes of $Pu^{VI}O_2^{2+}$ and $U^{VI}O_2^{2+}$ solutions for an examination and comparison of gas-phase reactions under similar experimental conditions [43].

Electronic supplementary material The online version of this article (https://doi.org/10.1007/s13361-018-1947-5) contains supplementary material, which is available to authorized users.

Correspondence to: Michael Stipdonk; *e-mail:* vanstipdonkm@duq.edu

More recent experiments by our group have demonstrated that the 2-D, linear ion trap (LIT) can provide access to fragmentation pathways and reactions not observed in earlier studies with 3-D ion traps [51–55]. For example, our past studies of the dissociation behavior of gas-phase actinyl complexes using a 3-D ion trap were complicated by high yields of product ions obviously generated by collisions with background H_2O. Relatively high levels of H_2O in the ion trap (ca. 10^{-6} Torr) create hydrated ions or lead to charge reduction reactions that form products such as $[U^{VI}O_2(OH)]^+$ and $[U^{V}O_2]^+$ and larger hydrated complexes containing these cations [6, 7, 43]. Ligand (H_2O) addition reaction rates were so fast that $U^{VI}O_2^{2+}$ cations coordinated by two or three aco ligands, generated by CID of larger precursors, hydrated to generate heterogeneous, tetra- or pentacoordinate complexes that dominated the product ion spectrum [6]. This prevented the detailed investigation of complex ions containing $U^{VI}O_2^{2+}$ and two or fewer ligands. However, a more recent investigation of the fragmentation behavior of $U^{VI}O_2^{2+}$ complexes containing acn [51] demonstrated that the lower partial pressures of background H_2O in the LIT allowed us to produce bare $U^{VI}O_2^{2+}$ by multiple-stage CID and generate an $NU^{VI}O^+$ product by CID of $[U^{VI}O_2(NC)]^+$. While gas-phase $NU^{VI}O^+$ had previously been created by insertion of U^+ into NO [56], our experiments demonstrated that the species can also be produced in a CID reaction via a putative cyanate intermediate. Similar experiments have now been conducted with aco-coordinated $U^{VI}O_2^{2+}$, and novel products such as $[U^{VI}O_2\text{-}HCO]^+$ and $[U^{VI}O_2\text{-}CH_2CH_3]^+$ have been identified using a combination of isotope labeling and high-resolution/high-accuracy mass measurements [52].

In one early study by our group that used a 3-D quadrupole ion trap instrument, multiple-stage tandem mass spectrometry (MS^n) was used to determine the dissociation pathways for several cationic species, generated by ESI, and composed of (1) the uranyl ion, (2) nitrate or hydroxide, and (3) water or alcohol [8]. In general, CID of the uranyl complexes resulted in elimination of coordinating water and alcohol ligands. For under-coordinated complexes containing nitrate and one or two coordinating alcohol ligands, the elimination of nitric acid was observed, leaving a uranyl alkoxide ion pair. For complexes with H_2O ligands, MS^n CID led to the generation of $[U^{VI}O_2(OH)]^+$ and $[U^{VI}O_2(NO_3)]^+$. Subsequent CID of $[U^{VI}O_2(OH)]^+$ produced $U^{V}O_2^+$. The base peak in the spectrum generated by the dissociation of $[U^{VI}O_2(NO_3)]^+$, however, was an H_2O adduct to $U^{V}O_2^+$. The abundance of the species was greater than expected based on previous experimental measurements of the (slow) hydration rate for $U^{V}O_2^+$ when stored in the ion trap [9]. To account for the production of $[U^{V}O_2(H_2O)]^+$ from $[U^{VI}O_2(NO_3)]^+$, a reaction involving collisions with water in the ion trap, with reductive elimination of NO_3, was proposed.

In the present study, the CID of these species was reexamined using the 2-D LIT employed in our most recent investigations, with the goal of determining whether additional, previously obscured dissociation pathways would be revealed under gas-phase conditions in which the level of residual H_2O was lower. As discussed below, the dominant product ion following CID of $[U^{VI}O_2(NO_3)]^+$ is $[U^{V}O_2(O_2)]^+$, rather than $[U^{V}O_2(H_2O)]^+$. To determine whether this result was due to the use of a different mass spectrometer, H_2O was deliberately added to the vacuum system of the LIT. Under conditions that included higher levels of background H_2O, CID of $[U^{VI}O_2(NO_3)]^+$ created $[U^{V}O_2(H_2O)]^+$ and $U^{V}O_2^+$, consistent with our earlier study using the 3-D ion trap [8]. No formation of $[U^{V}O_2(O_2)]^+$ was observed with the higher levels of residual H_2O. The experiments in the LIT allow for a revision of the previously proposed mechanism for the decomposition of $[U^{VI}O_2(NO_3)]^+$ to one that involves a two-step process: initial formation of $[U^{VI}O_2(O_2)]^+$ followed by rapid exchange of O_2 for H_2O by ion-molecule reaction. Our experiments further illustrate the extent to which the presence of residual H_2O in ion trap instruments influences dissociation patterns and pathways, and provide a more accurate description of the intrinsic dissociation pathway for $[U^{VI}O_2(NO_3)]^+$.

Experimental Methods

Sample Preparation

Uranyl nitrate hexahydrate ($U^{VI}O_2(NO_3)_2\bullet 6H_2O$) was purchased from Fluka/Sigma-Aldrich (St. Louis, MO) and used as received. Methanol (CH_3OH) and ethanol (CH_3CH_2OH) were purchased from Sigma-Aldrich Chemical (St. Louis, MO) and used as received. A stock solution (1×10^{-3} M) of $U^{VI}O_2(NO_3)_2\bullet 6H_2O$ was prepared by dissolving the appropriate amount of solid material in deionized H_2O. Because the uranyl nitrate solid is several years old, a "fresh" sample was also prepared by combining 2–3 mg of $U^{VI}O_3$ (Strem Chemicals, Newburyport, MA), corresponding to approximately 7×10^{-6} to 1×10^{-5} mol, with a twofold mole excess of nitric acid (Sigma Aldrich, St. Louis, MO) and 400 μL of deionized/distilled H_2O in a glass scintillation vial. The solution was allowed to incubate on a hot plate at 70 °C for 12 h. *Caution: uranium oxide is radioactive (α- and γ-emitter), and proper shielding, waste disposal, and personal protective gear should be used when handling the material.* When cooled, 20 μL of the resulting solution was diluted with 800 μL of 50:50 (by volume) H_2O/CH_3OH or H_2O/CH_3CH_2OH and used without further work up as the spray solution for ESI-MS.

ESI and CID experiments were performed on a ThermoScientific (San Jose, CA) LTQ-XL LIT mass spectrometer. The spray solutions were infused into the ESI-MS instrument using the incorporated syringe pump at a flow rate of 5 μL/min. In the positive ion mode, the atmospheric pressure ionization stack settings for the LTQ (lens voltages, quadrupole and octopole voltage offsets, etc.) were optimized for maximum transmission of singly charged ions such as $[U^{VI}O_2(NO_3)(CH_3OH)_3]^+$ and $[U^{VI}O_2(NO_3)(CH_3CH_2OH)_3]^+$ to the LIT by using the auto-tune routine within the LTQ Tune program. Helium was used as the bath/buffer gas to improve trapping efficiency and as the collision gas for CID experiments.

For CID, precursor ions were isolated using a width of 1.0 to 1.5 mass to charge (*m/z*) units. The exact value was determined empirically to provide maximum ion intensity while ensuring isolation of a single isotopic peak. To probe CID behavior in general, the (mass) normalized collision energy (NCE; as defined by ThermoScientific) was set between 5 and 18%, which corresponds to 0.075–0.27 V applied for CID with the current instrument calibration. The activation *Q*, which defines the frequency of the applied radio frequency potential, was set at 0.30 and the activation time employed was 30 ms. High-purity He (~ 1 mTorr in the LIT) was used as the collision gas.

To probe gas-phase reactions of selected precursor ions with background H_2O, ions were isolated using widths of 1–2 *m/z* units. Again, the specific width used was chosen empirically to ensure maximum ion isolation efficiency. The ions were then stored in the LIT for periods ranging from 1 ms to 10 s. Despite the lower H_2O levels in the 2-D LIT under normal operating conditions, there is still a sufficient partial pressure of the neutral to permit an investigation of ion-molecule reactions, particular when using long isolation times. For both CID and ion-molecule reaction (IMR) experiments, the mass spectra displayed were created by accumulating and averaging at least 30 isolation, dissociation, and ejection/detection steps.

Our instrument is not currently configured to allow the controlled introduction of neutral species into the LIT for detailed investigations of IMR. To increase the amount of background H_2O in the vacuum system, the instrument was turned off, the vacuum chamber vented, and held at room temperature and pressure for 12 h. After a pump down time of 3 h, CID experiments were performed using the same precursor ions using similar CID and IMR parameters, but under what we refer to in later sections as relatively "high" levels of residual H_2O. Though the partial pressure of H_2O in the ion trap is not known, as discussed later, evidence for higher H_2O levels was apparent in the CID product ion distributions.

Results and Discussion

As noted earlier, our previous study involved MS^n experiments with a 3-D ion trap instrument to determine the dissociation pathways for complexes containing $[U^{VI}O_2(NO_3)]^+$ coordinated by water or alcohol ligands [8]. The multiple-stage CID spectra initiated with the dissociation of, for example, $[U^{VI}O_2(NO_3)(CH_3OH)_3]$ were complex, and contained product ions from fragmentation reactions *and* H_2O adducts to those product ions formed by association reactions with H_2O present as a contaminant in the He buffer/bath gas. In the earlier experiments, the H_2O adducts were identified by characteristic peak tails and chemical mass shifts (shifts of 0.2–0.3 u lower than expected mass). It had been proposed that the asymmetric peak shapes and mass deficits may be tied to the formation of fragment ions from particularly "fragile" precursors because of the application of resonance ejection, and the magnitude of the resonant ejection amplitude for ion ejection during mass analysis using ion traps [57]. The ejection of the fragment ions, which "appears as premature ejection of the fragile ion, leads to the appearance of peak fronting and a mass shift" [57]. The reader is directed to reports by Yost and coworkers [57] and Vachet et al. [58], for specific details.

Formation of adducts can also be confirmed by isolating expected product ions in the ion trap for periods of 10–100 ms, without an applied collision voltage (NCE). During the isolation step, all ionized species except the one chosen for storage are resonantly ejected from the ion trap. The appearance of peaks 18 u higher than the isolated ion is indicative of the formation of H_2O adducts and their abundance increased as the isolation and storage time was extended.

The multiple-stage CID experiments initiated with the $[U^{VI}O_2(NO_3)(CH_3OH)_3]^+$ precursor ultimately generated $[U^{VI}O_2(OCH_3)]^+$ as the dominant product ion (through the elimination of HNO_3 from $[U^{VI}O_2(NO_3)(CH_3OH)]^+$). The relative intensity of $[U^{VI}O_2(NO_3)]^+$ produced by CID of $[U^{VI}O_2(NO_3)(CH_3OH)]^+$ was ~ 5%. In the same study, the MS^n CID of $[U^{VI}O_2(NO_3)(H_2O)_3]^+$ produced $[U^{VI}O_2(NO_3)]^+$, and subsequent dissociation of this species led to product ions at *m/z* 270 ($U^VO_2^+$) and *m/z* 288. Because there was no reasonable explanation for the elimination of 44 u from $[U^{VI}O_2(NO_3)]^+$, the product ion at *m/z* 288 was assigned as the hydrated, reduced uranyl ion, $[U^VO_2(H_2O)]^+$. CID of $[U^VO_2(H_2O)]^+$ caused the elimination of 18 u, consistent with the loss of H_2O to form $U^VO_2^+$ at *m/z* 270. Curiously, the *m/z* 288 product ion was significantly higher after CID of $[U^{VI}O_2(NO_3)]^+$ than when $U^VO_2^+$ was isolated independently for association reactions with H_2O, which leads to the conclusion that it was unlikely that the *m/z* 288 ion (produced by CID of $[U^{VI}O_2(NO_3)]^+$) resulted from addition of H_2O to the *m/z* 270 ($U^VO_2^+$) product ion by IMR. Instead, we proposed at the time that $[U^VO_2(H_2O)]^+$ was generated via reaction 1:

$$\left[U^{VI}O_2(NO_3)\right]^+ + H_2O \rightarrow \left[U^{VI}O_2NO_3(H_2O)\right]^{*+} \rightarrow \left[U^VO_2(H_2O)\right]^+ + NO_3^{\circ} \quad (1)$$

in which an energetic collision with H_2O in the ion trap mass causes the formation of an activated ternary complex, rapidly followed by the reductive elimination of NO_3 radical (with electron transfer to the uranyl ion) to leave the hydrated, reduced uranyl ion. It was this result in particular that prompted the study presented here.

The ESI and MS^n CID spectra collected on the 2-D LIT instrument, using a solution of (commercially available) uranyl nitrate in a mixture of H_2O and CH_3OH, are shown in Fig. 1. With this solution, ESI (Fig. 1a) generates $[U^{VI}O_2(OCH_3)(CH_3OH)_2]^+$, $[U^{VI}O_2(NO_3)(CH_3OH)_2]^+$, and $[U^{VI}O_2(NO_3)(CH_3OH)_3]^+$ at *m/z* 365, 396, and 428, respectively. CID of $[U^{VI}O_2(NO_3)(CH_3OH)_3]^+$ (MS/MS stage, Fig. 1b) causes elimination of a single CH_3OH ligand to produce

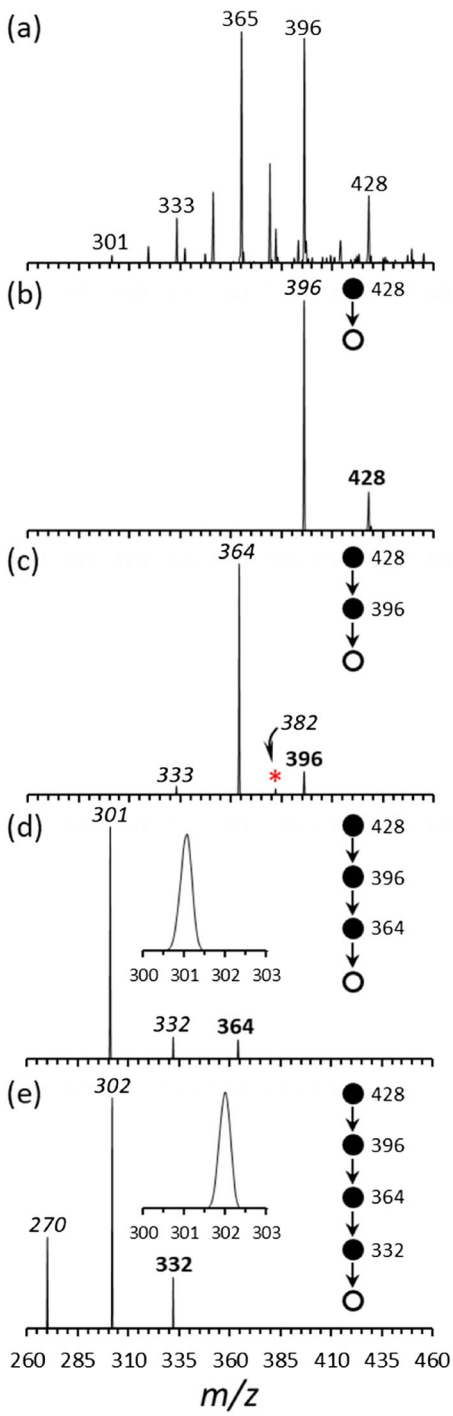

Figure 1. ESI and multiple-stage CID spectra derived from commercially available $UO_2(NO_3)_2 \bullet 6H_2O$ in 50:50 H_2O/CH_3OH, using "low" background H_2O conditions. (**a**) ESI-MS, (**b**) CID (MS/MS) of $[UO_2(NO_3)(CH_3OH)_3]^+$ at *m/z* 428, (**c**) CID (MS^3 stage) of $[UO_2(NO_3)(CH_3OH)_2]^+$ at *m/z* 396, (**d**) CID (MS^4 stage) of $[UO_2(NO_3)(CH_3OH)]^+$ at *m/z* 364, and (**e**) CID (MS^5 stage) of $[UO_2(NO_3)]^+$ at *m/z* 332. In each CID spectrum, the bold peak label indicates the precursor selected for CID while labels in italics represent the products from dissociation or ion-molecule reactions as indicated in the text. Filled circles correspond to species isolated for dissociation in the MS^n sequence. H_2O adducts to product ions are indicated with an asterisk

$[U^{VI}O_2(NO_3)(CH_3OH)_2]^+$, which in a subsequent stage (MS^3 stage, Fig. 1c) loses another CH_3OH ligand to create $[U^{VI}O_2(NO_3)(CH_3OH)]^+$ at *m/z* 364, or HNO_3 to leave $[U^{VI}O_2(OCH_3)(CH_3OH)]^+$ at *m/z* 333. Subsequent CID of $[U^{VI}O_2(NO_3)(CH_3OH)]^+$ (MS^4 stage, Fig. 1d) primarily causes the elimination of HNO_3 to leave $[U^{VI}O_2(OCH_3)]^+$ at *m/z* 301, and $[U^{VI}O_2(NO_3)]^+$ at *m/z* 332 was also observed at ~10% relative intensity. In general, the fragmentation reactions to this point are in agreement with our earlier study that used the 3-D ion trap [8]. However, one notable difference is that the number and intensity of H_2O adducts are greatly diminished in the present experiments, consistent with several recent studies by our group [51–55]. For example, the only adduct observed at relative intensity greater than 1% appears at *m/z* 382 (addition of H_2O to $[U^{VI}O_2(NO_3)(CH_3OH)]^+$ at *m/z* 364).

CID of $[U^{VI}O_2(OCH_3)]^+$ at *m/z* 301 (MS^5 stage, Fig. S1a) generates $U^VO_2^+$ at *m/z* 270 and $U^{VI}O_2H^+$ at *m/z* 271, in agreement with a recent comparison of the fragmentation pathways of $[U^{VI}O_2(OCH_3)]^+$ and $[U^{VI}O_2(OCH_2CH_3)]^+$ [54]. More importantly, CID of $[U^{VI}O_2(NO_3)]^+$ (MS^5 stage, Fig. 1e) generates $U^VO_2^+$ at *m/z* 270, and the dominant fragment ion appears at *m/z* 302. The neutral loss to make the ion at *m/z* 302 corresponds to 30 u, and given the composition of the precursor ($[U^{VI}O_2(NO_3)]^+$), it is reasonable to conclude that this corresponds to elimination of NO to leave an ion with a formula of UO_4^+ as shown in reaction 2.

$$\left[U^{VI}O_2(NO_3)\right]^+ \rightarrow \left[U^VO_4\right]^+ + \bullet NO \qquad (2)$$

This reaction pathway was not observed in our previous examination of the CID of H_2O and alcohol-coordinated $[U^{VI}O_2(NO_3)]^+$. Subsequent CID of UO_4^+ caused the formation of $U^VO_2^+$ by elimination of O_2 (MS^5 stage, Fig. S1b).

While the appearance of the ion at *m/z* 302 in the CID spectrum of $[U^{VI}O_2(NO_3)]^+$ was a surprise, generation of a product with a formula of UO_4 is not without precedent. For example, in a recent study of gas-phase binary and complex oxide anion molecules of protactinium and uranium, the oxalate species $[U^VO_2(C_2O_4)]^-$ exhibited the spontaneous replacement of the oxalate ligand by O_2 to leave $U^{VI}O_4^-$ and two CO_2 molecules [50]. Quantum chemical calculations suggested that the structure of $U^{VI}O_4^-$ includes a distorted $U^{VI}O_2^{2+}$ core coordinated in the equatorial plane by two equivalent O atoms. We note that a UO_4^- ion has also been observed in CID experiments initiated with precursor anions such as $[U^{VI}O_2(NO_3)_3]^-$, $[U^{VI}O_2(ClO_4)_3]^-$, and $[U^{VI}O_2(CH_3COO)_3]^-$ [40].

More important to the present study, a UO_4^+ cation was produced by Duncan and coworkers by laser vaporization and supersonic expansion and studied with infrared laser photodissociation spectroscopy using Ar atom pre-dissociation [59]. The IR action spectrum of $UO_4^+Ar_2$ was collected in the O=U=O and O=O stretching regions, and spectral and structure assignments were made with the assistance of high-level

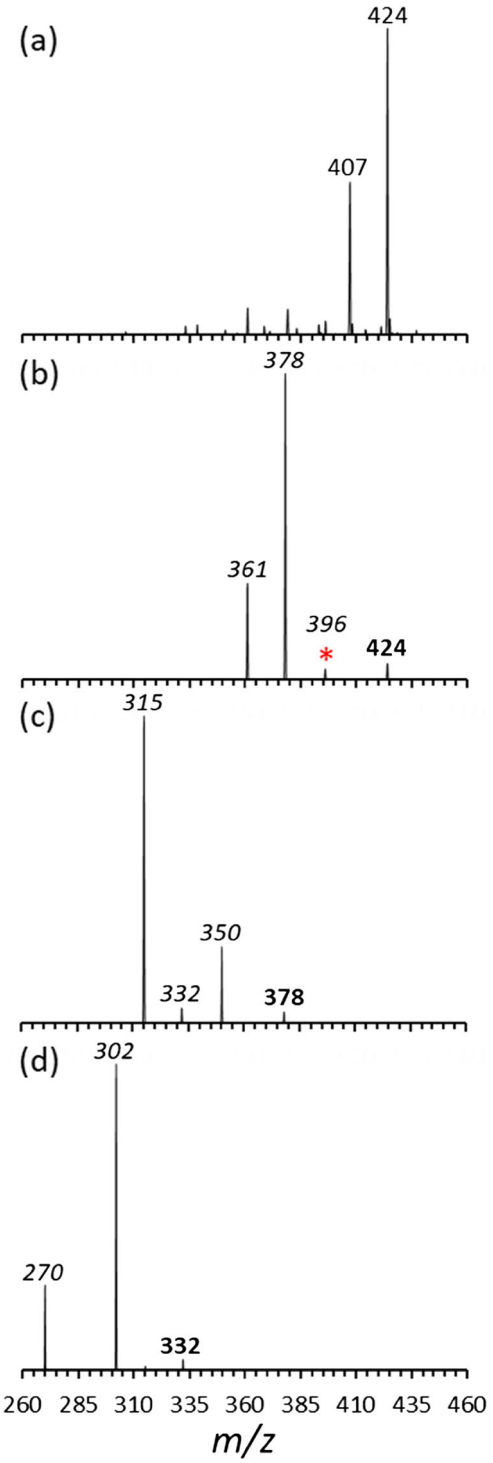

Figure 2. ESI and multiple-stage CID spectra derived from $UO_2(NO_3)_2$ (synthesized from UO_3) in 50:50 H_2O/CH_3CH_2OH, using "low" background H_2O conditions. (**a**) ESI-MS, (**b**) CID (MS/MS) of $[UO_2(NO_3)(CH_3CH_2OH)_2]^+$ at *m/z* 424, (**c**) CID (MS^3 stage) of $[UO_2(NO_3)(CH_3CH_2OH)]^+$ at *m/z* 378, and (**d**) CID (MS^4 stage) of $[U^{VI}O_2(NO_3)]^+$ at *m/z* 332. In each CID spectrum, the bold peak label indicates the precursor selected for CID while labels in italics represent the products from dissociation or ion-molecule reactions as indicated in the text. Filled circles correspond to species isolated for dissociation in the MS^n sequence. H_2O adducts to product ions are indicated with an asterisk

computational quantum chemistry. UO_4^+ was found to have a central U^VO_2 core, with O_2 bound side-on in a η^2 coordination mode, as suggested in previous experimental and theoretical studies of the addition of molecular O_2 to $U^VO_2^+$ complexes in the gas phase [60–63]. Therefore, the composition of the ion at *m/z* 302, created in the present study by CID of $[U^{VI}O_2(NO_3)]^+$, is assigned as $[U^VO_2(O_2)]^+$ and is assumed to have the structure revealed in the pre-dissociation experiments [59].

Formation of $[U^VO_2(O_2)]^+$ by CID in the LIT instrument was not dependent on the specific precursor used for the multiple-stage CID experiments. For example, multiple-stage CID initiated with either $[U^{VI}O_2(NO_3)(CH_3CH_2OH)_2]^+$ or $[U^{VI}O_2(NO_3)(H_2O)_2]^+$, using the commercially available nitrate salt, led to formation of $[U^{VI}O_2(NO_3)]^+$, which subsequently dissociated to leave $[U^VO_2(O_2)]^+$ and $U^VO_2^+$ (spectra not shown). We also investigated whether or not the formation of $[U^VO_2(O_2)]^+$ was an artifact of the uranyl nitrate starting material. The ESI and multiple-stage CID spectra resulting from the use of fresh uranyl nitrate synthesized from $U^{VI}O_3$ are shown in Fig. 2. The dominant ions generated by ESI using the synthetic salt in H_2O/CH_3CH_2OH were $[U^{VI}O_2(OCH_2CH_3)(CH_3CH_2OH)_2]^+$ and $[U^{VI}O_2(NO_3)(CH_3CH_2OH)_2]^+$ at *m/z* 407 and 424, respectively. CID of $[U^{VI}O_2(NO_3)(CH_3CH_2OH)_2]^+$ (MS/MS stage, Fig. 2b) caused the elimination of a CH_3CH_2OH ligand to leave $[U^{VI}O_2(NO_3)(CH_3CH_2OH)]^+$ at *m/z* 378, or loss of HNO_3 to generate $[U^{VI}O_2(OCH_2CH_3)(CH_3CH_2OH)]^+$ at *m/z* 361. Subsequent CID of $[U^{VI}O_2(OCH_2CH_3)(CH_3CH_2OH)]^+$ at *m/z* 361 created $[U^{VI}O_2(OCH_2CH_3)]^+$ at *m/z* 315 (spectrum not shown), consistent with our earlier investigation of uranyl alkoxide cations [54]. The dominant product ion generated by CID of $[U^{VI}O_2(NO_3)(CH_3CH_2OH)]^+$ at *m/z* 378 (MS^3 stage, Fig. 2c) was $[U^{VI}O_2OCH_2CH_3]^+$ at *m/z* 315, with $[UO_2(NO_3)]^+$ at *m/z* 332 appearing at a relative intensity of ~5%. CID of $[U^{VI}O_2(OCH_2CH_3)]^+$ (MS^5 stage, Fig. S1c) generated products such as $[U^VO_2(O{=}CH_2)]^+$, $[U^{VI}O_2(CH_3)]^+$, and $U^VO_2^+$ (*m/z* 300, 285, and 270, respectively), consistent with a previous study by our group using the LIT [54]. As with the other experiments performed with the LIT in this study, including those that used the commercially available salt, subsequent CID of $[U^{VI}O_2(NO_3)]^+$ (MS^4 stage, Fig. 2d) created $[U^VO_2(O_2)]^+$ and $U^VO_2^+$.

The last goal in this study was to determine whether the difference between the previous and current results, with respect to the dissociation of $[U^{VI}O_2(NO_3)]^+$, is due to the presence of significant levels of background H_2O, or the specific ion trap used in the MS^n experiment. As noted in the "Experimental Methods" section, the LIT was vented and kept at ambient temperature and pressure for 12 h. Our hypothesis was that the typical humidity of the ambient air would lead to relatively higher H_2O levels in the vacuum system and ion trap for a short period of time after pump down. Therefore, after the instrument returned to typical operating pressure (ca. 1.0×10^{-6} Torr in the vacuum chamber), the MS^n experiment using ethanol-coordinated $[U^{VI}O_2(NO_3)]^+$ was repeated to make a direct comparison to the experiments run under the "low" H_2O

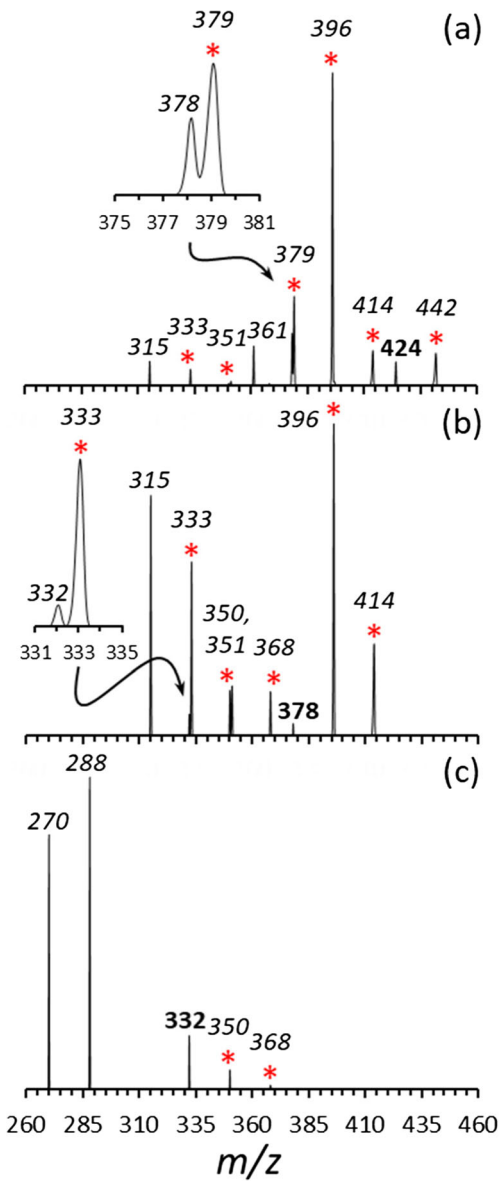

Figure 3. ESI and multiple-stage CID spectra derived from $UO_2(NO_3)_2$ (synthesized from UO_3) in 50:50 H_2O/CH_3CH_2OH, using "high" background H_2O conditions. (**a**) ESI-MS, (**b**) CID (MS/MS) of $[UO_2(NO_3)(CH_3CH_2OH)_2]^+$ at *m/z* 424, (**c**) CID (MS^3 stage) of $[UO_2(NO_3)(CH_3CH_2OH)]^+$ at *m/z* 378, and (**d**) CID (MS^4 stage) of $[U^{VI}O_2(NO_3)]^+$ at *m/z* 332. In each CID spectrum, the bold peak label indicates the precursor selected for CID while labels in italics represent the products from dissociation or ion-molecule reactions as indicated in the text. Filled circles correspond to species isolated for dissociation in the MS^n sequence. H_2O adducts to product ions are indicated with an asterisk

level conditions. The CID spectra, initiated using the $[U^{VI}O_2(NO_3)(CH_3CH_2OH)_2]^+$ precursor, are provided in Fig. 3.

Under the high H_2O conditions, the dominant product ion observed following CID of $[U^{VI}O_2(NO_3)(CH_3CH_2OH)_2]^+$ (MS/MS stage, Fig. 3a) appears at *m/z* 396 (throughout Fig. 3, H_2O adducts to CID product ions are indicated with an asterisk). The product ion at *m/z* 396 corresponds to the H_2O adduct to $[U^{VI}O_2(NO_3)(CH_3CH_2OH)]^+$ (*m/z* 378). Other true dissociation products at the MS/MS stage include $[U^{VI}O_2(OCH_2CH_3)(CH_3CH_2OH)]^+$ at *m/z* 361 and $[U^{VI}O_2(OCH_2CH_3)]^+$ at *m/z* 315. Prominent H_2O adducts to these fragment ions appear at *m/z* 442, 414, 379, 351, and 333, demonstrating that the level of background H_2O was indeed higher.

Subsequent CID of $[U^{VI}O_2(NO_3)(CH_3CH_2OH)]^+$ at *m/z* 378 (MS^3 stage, Fig. 3b) primarily generated $[U^{VI}O_2(OCH_2CH_3)]^+$ at *m/z* 315 and mono and di-hydrates of the ion at *m/z* 333 and 351. The $[U^{VI}O_2(NO_3)]^+$ ion was also generated at nearly the same relative intensity as in the low H_2O conditions. In contrast to the experiments under low H_2O conditions, subsequent CID of $[U^{VI}O_2(NO_3)]^+$ (Fig. 3c, MS^4 stage) under the high H_2O conditions produced $[U^VO_2(H_2O)]^+$ at *m/z* 288 and $U^VO_2^+$ at *m/z* 270, exactly the results obtained in our previous investigation using the 3-D ion trap [8]. This result strongly suggests that the differences in product ion formation are not due to the specific ion trap used for the experiments, but instead to the presence of higher levels of background H_2O in the earlier study.

One additional hypothesis tested was that $[U^VO_2(O_2)]^+$ would undergo a ligand exchange reaction with H_2O. Our motivation for this was a set of earlier studies by our group which showed that (a) gas-phase complexes containing $U^VO_2^+$ ligated with two or three σ-donating acetone ligands react with O_2 to form complexes with composition $[U^VO_2(A)_{2,3}(O_2)]^+$ (A = acetone, acetonitrile, etc.) [60–62] and (b) the O_2 ligand is easily eliminated by CID or exchanges for neutral ligands such as H_2O, acetone, or acetonitrile by IMR [62].

Using the relatively low residual H_2O conditions in the LIT, the ion at *m/z* 302 (presumed to be $[U^VO_2(O_2)]^+$) was generated by MS^n CID of the $[U^{VI}O_2(NO_3)(CH_3CH_2OH)_2]^+$ precursor, and then isolated and allowed to react with background H_2O for periods ranging from 10 to 1000 msec (Fig. 4a–c). Despite the low levels of background H_2O, reactions with the neutral species can still be observed, especially when using relatively long isolation/reaction times. The spectra shown in Fig. 4a–c clearly show that the product ion generated by IMR appears at *m/z* 288, consistent with the exchange of O_2 for H_2O by reaction 3.

$$\left[U^VO_2(O_2)\right]^+ + H_2O \rightarrow \left[U^VO_2(H_2O)\right]^+ + O_2 \qquad (3)$$

Subsequent CID (Fig. 4d) of the ion at *m/z* 288 causes formation of $U^VO_2^+$ by loss of H_2O. This behavior is therefore consistent with our earlier studies of ligand exchange reactions of O_2 adducts to $U^VO_2^+$ complexes, and with the composition assignment of $[U^VO_2(O_2)]^+$ for the *m/z* 302 ion.

One remaining question is the mechanism by which NO is released from $[U^{VI}O_2(NO_3)]^+$ to make $[U^VO_2(O_2)]^+$. A study by Frański [64] showed that NO is eliminated from Ca^{2+}, Sr^{2+}, and Ba^{2+} complexes with nitrate, but mechanistic details and energetics were not provided. Schröder and coworkers [65] demonstrated that decomposition of nitrate will occur for gas-

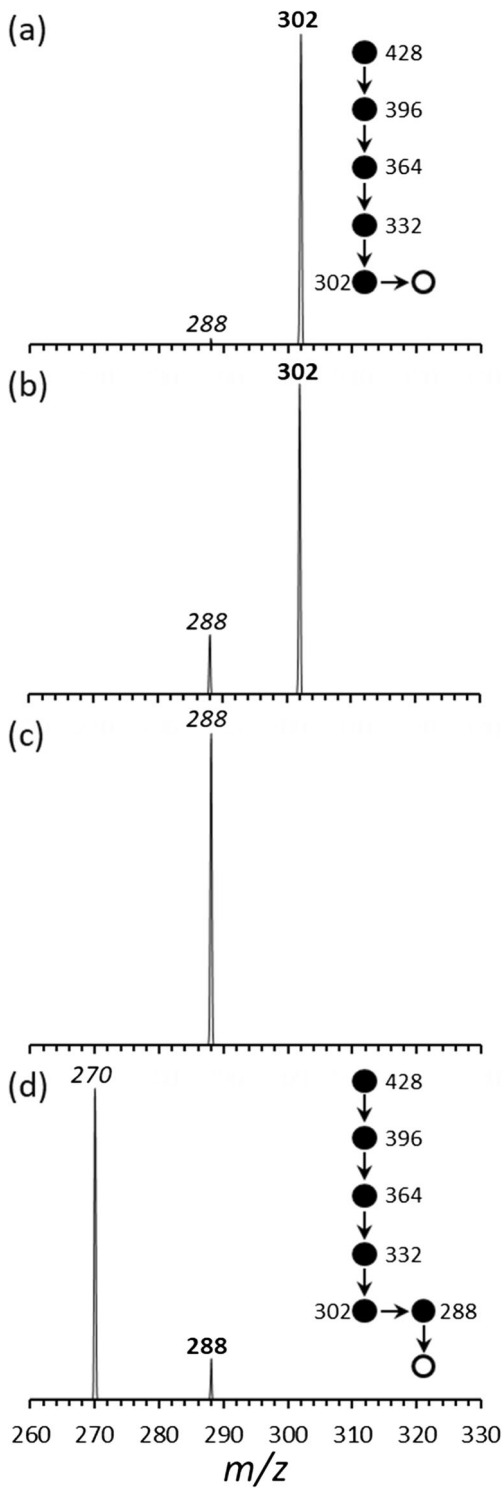

Figure 4. Product ion spectra derived from isolation of $[UO_2(O_2)]^+$ for reaction with background H_2O. (**a**) 10 msec isolation time, (**b**) 100 msec isolation time, and (**c**) 1 s isolation time. (**d**) CID of *m/z* 288 species generated by ligand (H_2O for O_2) exchange reaction. Filled circles correspond to species isolated for ion-molecule reaction or CID in the MS^n sequence

phase complexes of Co and Ni. For the case of Co, NO^+ was observed and attributed to the dissociation of $[CoNO_3]^+$. For the Ni system, loss of (neutral) NO was observed from the mono-hydrate of $[NiNO_3]^+$. An alternative to direct ejection of NO would be isomerization of nitrate to peroxynitrite (reaction 4), followed by decomposition and elimination of (neutral) NO.

$$\left[U^{VI}O_2(NO_3)\right]^+ \rightarrow \left[U^{VI}O_2O_2NO\right]^+ \rightarrow \left[U^{V}O_2(O_2)\right]^+ + \bullet NO \quad (4)$$

This is the reverse of the well-known isomerization of peroxynitrite to nitrate (and hydrogen peroxynitrite to nitric acid) after creation of the former by reaction of NO and superoxide ion [66–70]. The exact mechanism by which $[U^{V}O_2(O_2)]^+$ is generated in the present study remains unclear and would benefit from a detailed quantum chemical study. Whatever the mechanism, our results strongly suggest that the decomposition of $[U^{VI}O_2(NO_3)]^+$ involves the initial elimination of NO.

Conclusions

To summarize, in this study, we revisited the dissociation of complexes composed of uranyl nitrate cation $[U^{VI}O_2(NO_3)]^+$ coordinated by alcohol ligands (methanol and ethanol) using the 2-D LIT. With relatively low levels of background H_2O, CID of $[U^{VI}O_2(NO_3)]^+$ primarily creates $[U^{V}O_2(O_2)]^+$ by the ejection of NO (reaction 2). However, under conditions in which the level of residual H_2O is higher, CID of $[U^{VI}O_2(NO_3)]^+$ instead leads to formation of $[U^{V}O_2(H_2O)]^+$ and $U^{V}O_2^+$, consistent with our earlier investigation of similar systems on a 3-D quadrupole ion trap. Our experiments further illustrate the impact of residual H_2O in ion trap instruments on the product ions generated by CID and reveal the correct dissociation pathway for $[U^{VI}O_2(NO_3)]^+$.

Based on these new results, we can revise the apparent intrinsic dissociation reaction for $[U^{VI}O_2(NO_3)]^+$. It is reasonable to assume that CID of $[U^{VI}O_2(NO_3)]^+$ initially creates $[U^{V}O_2(O_2)]^+$ by elimination of NO (reaction 2). The $[U^{V}O_2(O_2)]^+$ product can further dissociate by loss of O_2 to leave $U^{V}O_2^+$, consistent with the dissociation pattern observed on the LIT instrument. Knowing that $[U^{V}O_2(O_2)]^+$ can undergo a spontaneous and rapid exchange of O_2 for H_2O (reaction 3), the earlier results on the 3-D ion trap may have involved a two-step process: the initial formation of $[U^{V}O_2(O_2)]^+$, followed by rapid exchange with H_2O to leave the species at *m/z* 288. This is essentially reactions 2 and 3 in rapid succession. Both $[U^{V}O_2(O_2)]^+$ and $[U^{V}O_2(H_2O)]^+$ may dissociate to leave $U^{V}O_2^+$ at *m/z* 270. We therefore conclude that dissociation reactions in our previous study using the 3-D trap were influenced by the relatively high levels of residual H_2O, and the results obtained on the 2-D ion trap more accurately reflect the intrinsic CID pathway for $[U^{VI}O_2(NO_3)]^+$.

Funding Information MVS received support for this work in the form of start-up funds from the Bayer School of Natural and Environmental Sciences and Duquesne University. Laboratory space renovation was made possible with support from the National Science Foundation through grant CHE-0963450. This work was also supported in part by the Robert Dean Loughney Faculty Development Endowment.

References

1. Weigel, F.: In: Katz, J.J., Morss, L.R., Seaborg, G.T. (eds.) The Chemistry of the actinide elements, p. 169. Chapman and Hall, London (1986)
2. Greenwood, N.N., Earnshaw, A.: Chemistry of the elements. Butterworth Heinemann, Oxford (1997)
3. Murphy, W.M., Shock, E.L.: Uranium: mineralogy, geochemistry and the environment. In: Burns, P.C., Finch, R. (eds.) , p. 221. Mineralogical Society of America, Washington, D. C. (1999)
4. Brookins, D.G.: Geochemical aspects of radioactive waste disposal. Springer-Verlag, New York (1984)
5. Agnes, G.R., Horlick, G.: Electrospray mass spectrometry as a technique for elemental analysis: preliminary results. Appl. Spectrosc. **46**, 401–406 (1992)
6. Van Stipdonk, M.J., Chien, W., Anbalagan, V., Bulleigh, K., Hanna, D., Groenewold, G.: Gas-phase complexes containing the uranyl ion and acetone. J. Phys. Chem. A. **108**, 10448–10457 (2004)
7. Stipdonk, V., Chien, M.J., Bulleigh, W., Wu, K., Groenewold, Q., S, G.: Gas-phase uranyl-nitrile complex ions. J. Phys. Chem. A. **110**, 959–970 (2006)
8. Van Stipdonk, M., Gresham, G., Groenewold, G., Anbalagan, V., Hanna, D., Chien, W.: Elucidation of the collision-induced dissociation pathways of water and alcohol coordinated complexes containing the uranyl cation. J. Am. Soc. Mass Spectrom. **14**, 1205–1214 (2003)
9. Chien, W., Hanna, D., Anbalagan, V., Gresham, G., Groenewold, G., Zandler, M., Van Stipdonk, M.: Intrinsic hydration of uranyl-hydroxide, -nitrate and -acetate complexes. J. Am. Soc. Mass Spectrom. **15**, 777–783 (2004)
10. Groenewold, G.S., Van Stipdonk, M.J., Gresham, G.L., Chien, W., Bulleigh, K., Howard, A.: CID MS/MS of desferrioxamine siderophore complexes from ESI of UO_2^{2+}, Fe^{3+} and Ca^{2+} solutions. J. Mass Spectrom. **39**, 752–761 (2004)
11. Van Stipdonk, M., Chien, W., Anbalagan, V., Gresham, G.L., Groenewold, G.S.: Oxidation of 2-propanol ligands during collision-induced dissociation of a gas-phase uranyl complex. Int. J. Mass Spectrom. **237**, 175–183 (2004)
12. Groenewold, G.S., Gianotto, A.K., Cossel, K.C., Van Stipdonk, M.J., Moore, D.T., Polfer, N., Oomens, J., de Jong, W.A., Visscher, L.: Vibrational spectroscopy of mass-selected $[UO_2(ligand)_n]^{2+}$ complexes in the gas phase: comparison with theory. J. Am. Chem. Soc. **128**, 4802–4813 (2006)
13. Groenewold, G.S., Oomens, J., de Jong, W.A., Gresham, G.L., McIlwain, M.E., Van Stipdonk, M.J.: Vibrational spectroscopy of anionic nitrate complexes of UO_2^{2+} and Eu^{3+} isolated in the gas phase. Phys. Chem. Chem. Phys. **10**, 1192–1202 (2008)
14. Groenewold, G.S., Van Stipdonk, M.J., de Jong, W.A., Oomens, J., Gresham, G.L., McIlwain, M.E., Gao, D., Siboulet, B., Visscher, L., Kullman, M., Polfer, N.: Infrared spectroscopy of dioxouranium(V) complexes with solvent molecules: effect of reduction. ChemPhysChem. **9**, 1278–1285 (2008)
15. Groenewold, G.S., van Stipdonk, M.J., Oomens, J., de Jong, W.A., McIlwain, M.E.: The gas-phase bis-uranyl nitrate complex $[(UO_2)_2(NO_3)_5]^-$: infrared spectrum and structure. Int. J. Mass Spectrom. **308**, 175–180 (2011)
16. Tsierkezos, N.G., Roithova, J., Schroder, D., Oncak, M., Slavicek, P.: Can electrospray mass spectrometry quantitatively probe speciation? Hydrolysis of uranyl nitrate studied by gas-phase methods. Inorg. Chem. **48**, 6287–6296 (2009)
17. Pasilis, S.P., Pemberton, J.E.: Speciation and coordination chemistry of uranyl(VI)-citrate complexes in aqueous solution. Inorg. Chem. **42**, 6793–6800 (2003)
18. Pasilis, S., Somogyi, Á., Herrmann, K., Pemberton, J.E.: Ions generated from uranyl nitrate solutions by electrospray ionization (ESI) and detected with Fourier transform ion-cyclotron resonance (FT-ICR) mass spectrometry. J. Am. Soc. Mass Spectrom. **17**, 230–240 (2006)
19. Somogyi, A., Pasilis, S.P., Pemberton, J.E.: Electrospray ionization of uranyl-citrate complexes: adduct formation and ion-molecule reactions in a 3D ion trap and ion cyclotron resonance trapping instruments. Int. J. Mass Spectrom. **265**, 281–294 (2007)
20. Mustapha, A.J., Pasilis, S.P.: Probing uranyl(VI) speciation in the presence of amidoxime ligands using electrospray ionization mass spectrometry. Rapid Commun. Mass Spectrom. **27**, 2135–2142 (2013)
21. Mustapha, A.J., Pasilis, S.P.: Gas-phase complexes formed between amidoxime ligands and vanadium or iron investigated using electrospray ionization mass spectrometry. Rapid Commun. Mass Spectrom. **30**, 1763–1770 (2016)
22. Schoendorff, G., de Jong, W.A., Van Stipdonk, M.J., Gibson, J.K., Rios, D., Gordon, M.S., Windus, T.L.: On the formation of "hypercoordinated" uranyl complexes. Inorg. Chem. **50**, 8490–8493 (2011)
23. Rios, D., Schoendorff, G., Van Stipdonk, M.J., Gordon, M.S., Windus, T.L., Gibson, J.K., de Jong, W.A.: Roles of acetone and diacetone alcohol in coordination and dissociation reactions of uranyl complexes. Inorg. Chem. **51**, 12768–12775 (2012)
24. Gong, Y., de Jong, W.A., Gibson, J.K.: Gas-phase uranyl activation: formation of a uranium nitrosyl complex from uranyl azide. J. Am. Chem. Soc. **137**, 5911–5915 (2015)
25. Jaison, P.G., Kumar, P., Telmore, V.M., Aggarwai, S.K.: Electrospray ionization mass spectrometric studies on uranyl complex with α-hydroxyisobutyric acid in water-methanol solution. Rapid Commun. Mass Spectrom. **27**, 1105–1118 (2013)
26. Kumar, P., Jaison, P.G., Telmore, V.M., Alamelu, D., Aggarwai, S.K., Sadhu, B., Sundararajan, M.: J. Radioanal. Nucl. Chem. **308**, 303–310 (2016)
27. Kumar, P., Jaison, P.G., Telmore, V.M., Sadhu, B., Sundararajan, M.: Speciation of uranium-mandelic acid complexes using electrospray ionization mass spectrometry and density functional theory. Rapid Commun. Mass Spectrom. **31**, 561–571 (2017)
28. Cametti, M., Ilander, L., Rissanen, K.: Recognition of Li^+ by a salophen-UO_2 homodimeric complex. Inorg. Chem. **48**, 8632–8637 (2009)
29. Galindo, C., Del Nero, M.: Trace level uranyl complexation with phenylphosphonic acid in aqueous solution: direct speciation by high resolution mass spectrometry. Inorg. Chem. **52**, 4372–4383 (2013)
30. Crawford, C.L., Fugate, G.A., Cable-Dunlap, P.R., Wall, N.A., Siems, W.F., Hill Sr., H.H.: The novel analysis of uranyl compounds by electrospray-ion mobility-mass spectrometry. Int. J. Mass Spectrom. **333**, 21–26 (2013)
31. McGrail, B.T., Sigmon, G.E., Jouffret, L.J., Andrews, C.R., Burns, P.C.: Raman spectroscopic and ESI-MS characterization of uranyl peroxide cage clusters. Inorg. Chem. **53**, 1562–1569 (2014)
32. Xiao, C.-L., Wang, C.-Z., Mei, L., Zhange, Z.-R., Wall, N., Zhao, Y.-L., Chai, Z.-F., Shi, W.-Q.: Europium, uranyl and thorium-phenanthroline amide complexes in acetonitrile solution: and ESI-MS and DFT combined investigation. Dalton Trans. **44**, 14376–14387 (2015)
33. Qin, Z., Shi, S., Yang, C., Wen, J., Jia, J., Zhang, Z., Yu, H., Wang, X.: The coordination of amidoxime ligands with uranyl in the gas-phase: a mass spectrometry and DFT study. Dalton Trans. **45**, 16413–16421 (2016)
34. McDonald, L.W., Campbell, J.A., Vercouter, T., Clark, S.B.: Characterization of actinides complexes to nuclear fuel constituents using ESI-MS. Anal. Chem. **88**, 2614–2621 (2016)
35. Das, D., Kannan, S., Maity, D.K., Drew, M.G.B.: Steric effects on uranyl complexation: synthetic, structural, and theoretical studies of carbamoyl pyrazole compounds of the uranyl(VI) ion. Inorg. Chem. **51**, 4869–4876 (2012)
36. Dau, P.D., Su, J., Liu, H.-T., Huang, D.-L., Li, J., Wang, L.-S.: Photoelectron spectroscopy and the electronic structure of the uranyl tetrachloride dianion: $UO_2Cl_4^{2-}$. J. Chem. Phys. **137**, 064315 (2012)
37. Dau, P.D., Su, J., Liu, H.-T., Liu, J.-B., Huang, D.-L., Li, J., Wang, L.-S.: Observation and investigation of the uranyl tetrafluoride dianion ($UO_2F_4^{2-}$) and its solvation complexes with water and acetonitrile. Chem. Sci. **3**, 1137–1146 (2012)
38. Li, W.-L., Su, J., Jian, T., Lopez, G.V., Hu, H.-S., Cao, G.-J., Li, J., Wang, L.-S.: Strong electron correlation in UO_2^-: a photoelectron spectroscopy and relativistic quantum chemistry study. J. Chem. Phys. **140**, 094306 (2014)
39. Su, J., Dau, P.D., Qiu, Y.-H., Liu, H.-T., Xu, C.-F., Huang, D.-L., Wang, L.-S., Li, J.: Probing the electronic structure and chemical bonding in tricoordinate uranyl complexes $UO_2X_3^-$ (X = F, Cl, Br, I): competition

between coulomb repulsion and U–X bonding. Inorg. Chem. **52**, 6617–6626 (2013)
40. Sokalaska, M., Prussakowska, M., Hoffmann, M., Gierczyk, B., Frański, R.: Unusial UO_4^- formed upon collision induced dissociation of $[UO_2(NO_3)_3]^-$, $[UO_2(ClO_4)_3]^-$, $[UO_2(CH_3COO)_3]^-$ ions. J. Am. Soc. Mass Spectrom. **21**, 1789–1794 (2010)
41. Luo, M., Hu, B., Zhang, X., Peng, D., Chen, H., Zhang, L., Huan, Y.: Extractive electrospray ionization mass spectrometry for sensitive detection of uranyl species in natural water samples. Anal. Chem. **82**, 282–289 (2010)
42. Rios, D., Michelini, M.C., Lucena, A.F., Marçalo, J., Gibson, J.K.: On the origins of faster oxo exchange for uranyl(V) versus plutonyl(V). J. Am. Chem. Soc. **134**, 15488–15496 (2012)
43. Rios, D., Rutkowski, P.X., Van Stipdonk, M.J., Gibson, J.K.: Gas-phase coordination complexes of dipositive plutonyl, PuO_2^{2+}: chemical diversity across the actinyl series. Inorg. Chem. **50**, 4781–4790 (2011)
44. Rios, D., Rutkowski, P.X., Shuh, D.K., Bray, T.H., Gibson, J.K., Van Stipdonk, M.J.: Electron transfer dissociation of dipositive uranyl and plutonyl coordination complexes. J. Mass Spectrom. **46**, 1247–1254 (2011)
45. Rutkowski, P.X., Rios, D., Gibson, J.K., Van Stipdonk, M.J.: Gas-phase coordination complexes of $U^{VI}O_2^{2+}$, $Np^{VI}O_2^{2+}$, and $Pu^{VI}O_2^{2+}$ with dimethylformamide. J. Am. Soc. Mass Spectrom. **22**, 2042–2048 (2011)
46. Rios, D., Michelini, M.C., Lucena, A.F., Marçalo, J., Bray, T., Gibson, J.K.: Gas-phase uranyl, neptunyl and plutonyl: hydration and oxidation studied by experiment and theory. Inorg. Chem. **51**, 6603–6614 (2012)
47. Gong, Y., Hu, H.-S., Rao, L., Li, J., Gibson, J.K.: Experimental and theoretical studies on the fragmentation of gas-phase uranyl, neptunyl and plutonyl-diglycolamide complexes. J. Phys. Chem. A. **117**, 10544–10550 (2013)
48. Gong, Y., Gibson, J.K.: Crown ether complexes of uranyl, neptunyl and plutonyl: hydration differentiates inclusion versus other coordination. Inorg. Chem. **11**, 5839–5844 (2014)
49. Dau, P.D., Rios, D., Gong, Y., Michelini, M.C., Marçalo, J., Shuh, D.K., Mogamman, M., Van Stipdonk, M.J., Corcovilos, T.A., Martens, J.K., Oomens, J., Redlich, B., Gibson, J.K.: Synthesis and hydrolysis of uranyl, neptunyl and plutonyl gas-phase complexes exhibiting discrete actinide-carbon bonds. Organometallics. **35**, 1228–1240 (2016)
50. de Jong, W.A., Dau, P., Wilson, R., Marçalo, J., Van Stipdonk, M.J., Corcovilos, T., Berden, G., Martens, J., Oomens, J., Gibson, J.K.: Revealing disparate chemistries of protactinium and uranium. Synthesis of the molecular uranium tetroxide anion, UO_4. Inorg. Chem. **56**, 3686–3694 (2017)
51. Van Stipdonk, M.J., del Carmen Michelini, M., Plaviak, A., Martin, D., Gibson, J.K.: Formation of bare UO_2^{2+} and NUO^+ by fragmentation of gas-phase uranyl-acetonitrile complexes. J. Phys. Chem. A. **118**, 7838–7846 (2014)
52. Van Stipdonk, M.J., O'Malley, C., Plaviak, A., Martin, D., Pestok, J., Mihm, P.A., Hanley, C.G., Corcovilos, T.A., Gibson, J.K., Bythell, B.J.: Dissociation of gas-phase, doubly-charged uranyl-acetone complexes by collisional activation and infrared photodissociation. Int. J. Mass Spectrom. **396**, 22–34 (2016)
53. Perez, E., Hanley, C., Koehler, S., Pestok, J., Polonsky, N., Van Stipdonk, M.: Gas phase reactions of ions derived from anionic uranyl formate and uranyl acetate complexes. J. Am. Soc. Mass Spectrom. **27**, 1989–1998 (2016)
54. Van Stipdonk, M.J., Hanley, C., Perez, E., Pestok, J., Mihm, P., Corcovilos, T.A.: Collision-induced dissociation of uranyl-methoxide and uranyl-ethoxide cations: formation of UO_2H^+ and uranyl-alkyl product ions. Rapid Commun. Mass Spectrom. **30**, 1879–1890 (2016)
55. Van Stipdonk, M., Bubas, A., Tatosian, I., Perez, E., Polonsky, N., Metzler, L., Somogyi, A.: Formation of $[U^VOF_4]^-$ by collision-induced dissociation of a $[U^{VI}O_2(O_2)(O_2C\text{-}CF_3)_2]^-$ precursor. Int. J. Mass Spectrom. **424**, 58–64 (2018)
56. Heinemann, C., Schwarz, H.: NUO^+, a new species isoelectronic to the uranyl dication UO_2^{2+}. Chem. Eur. J. **1**, 7–11 (1995)
57. McClellan, J.E., Murphy III, J.P., Mulholland, J.J., Yost, R.A.: Effects of fragile ions on mass resolution and on isolation for tandem mass spectrometry in the quadrupole ion trap mass spectrometer. Anal. Chem. **74**, 402–412 (2002)
58. Vachet, R.W., Hartmann, J.A.R., Callahan, J.H.: Ion-molecule reactions in a quadrupole ion trap as a probe of the gas-phase structure of metal complexes. J. Mass Spectrom. **33**, 1209–1225 (1998)
59. Ricks, A.M., Gagliardi, L., Duncan, M.A.: Uranium oxo and superoxo cations revealed using infrared spectroscopy in the gas phase. J. Phys. Chem. Lett. **2**, 1662–1666 (2011)
60. Groenewold, G.S., Cossel, K.C., Gresham, G.L., Gianotto, A.K., Appelhans, A.D., Olson, J.E., Van Stipdonk, M.J., Chien, W.: Binding of molecular O_2 to Di- and tri-ligated $[UO_2]^+$. J. Am. Chem. Soc. **128**, 3075–3084 (2006)
61. Bryantsev, V.S., Cossel, K.C., Diallo, M.S., Goddard III, W.A., de Jong, W.A., Groenewold, G.S., Chien, W., Van Stipdonk, M.J.: 2-Electron 3-atom bond in side-on (η_2) superoxo complexes: U(IV) and U(V) dioxo monocations. J. Phys. Chem. A. **112**, 5777–5780 (2008)
62. Leavitt, C.M., Bryantsev, V.S., de Jong, W.A., Diallo, M.S., Goddard III, W.A., Groenewold, G.S., Van Stipdonk, M.J.: Addition of H_2O and O_2 to acetone and dimethylsulfoxide ligated uranyl(V) dioxocations. J. Phys. Chem. A. **113**, 2350–2358 (2009)
63. Lucena, A.F., Carretas, J.M., Marçalo, J., Michelini, M.C., Gong, Y., Gibson, J.K.: Gas-phase reactions of molecular oxygen with uranyl(V) anionic complexes—synthesis and characterization of new superoxides of uranyl(VI). J. Phys. Chem. A. **119**, 3628–3635 (2015)
64. Frański, R.: Mass spectrometric decomposition of $[MNO_3]^+$ cations, where M=Ca, Sr, Ba. Polyhedron. **91**, 136–140 (2015)
65. Schröder, D., de Jong, K.P., Roithova, J.: Gas-phase model studies relevant to the decomposition of transition-metal nitrates $M(NO_3)_2$ (M=Co, Ni) into metal-oxo species. Eur. J. Inorg. Chem. **2009**, 2121–2128 (2009)
66. Manuszak, M., Koppenol, W.H.: The enthalpy of isomerization of peroxynitrite to nitrate. Thermochim. Acta. **273**, 11–15 (1996)
67. Jursic, B.S., Klasinc, L., Pecur, S., Pryor, W.A.: On the mechanism of HOONO to $HONO_2$ conversion. Nitric. Oxide Biol. Chem. **1**, 494–501 (1997)
68. Herold, S., Kalinga, S., Matsui, T., Watanabe, Y.: Mechanistic studies of the isomerization of peroxynitrite to nitrate catalyzed by distal histidine metmyoglobin mutants. J. Am. Chem. Soc. **126**, 6945–6955 (2004)
69. Contreras, R., Galván, M., Oliva, M., Safont, V., Andrés, J., Guerra, D., Aizman, A.: Two state reactivity mechanism for the rearrangement of hydrogen peroxynitrite to nitric acid. Chem. Phys. Lett. **457**, 216–221 (2008)
70. Ascenzi, P., Leboffe, L., Pesce, A., Ciaccio, C., Sbardella, D., Bolognesi, M., Coletta, M.: Nitrite-reductase and peroxynitrite isomerization activities of *Methanosarcina acetivorans* protoglobin. PLoS One. **9**, e95391 (2014)